PARTIAL RESPONSE CODING IN DIGITAL SUBSCRIBER LOOPS

by

N-S. Lin, D. A. Hodges and D. G. Messerschmitt

Memorandum No. UCB/ERL M85/37

6 May 1985

PARTIAL RESPONSE CODING IN DIGITAL SUBSCRIBER LOOPS

by

N.-S. Lin, D. A. Hodges and D. G. Messerschmitt

Memorandum No. UCB/ERL M85/37

6 May 1985

ELECTRONICS RESEARCH LABORATORY

College of Engineering
University of California, Berkeley
94720

PARTIAL RESPONSE CODING IN DIGITAL SUBSCRIBER LOOPS

Nan-Sheng Lin, D. A. Hodges, & D. G. Messerschmitt
Department of Electrical Engineering and Computer Sciences
and the Electronics Research Laboratory
UNIVERSITY OF CALIFORNIA, BERKELEY
BERKELEY, CALIFORNIA 94720

1. ABSTRACT

The performance of the echo canceller in a hybrid-mode system depends very much on the accuracy of the recovered timing phase. It has been shown that 60dB echo cancellation requires that the magnitude of jitter be smaller than 60dB. This is difficult even if an analog phase locked loop is used because it requires very narrow bandwidth. Besides, digital phase locked loop is much more desirable due to the simplicity of VLSI implementation compared with its analog counterpart. It is, however, very difficult to have the magnitude of jitter smaller than 60dB for a digital phase locked loop.

The use of an *interpolation technique* in conjunction with *modified duobinary partial response coding (PRC)* can greatly relax the requirement on the magnitude of the maximum jitter and, as a result, ease the design of the digital phase locked loop. The effect of partial response coding on the crosstalk interference in a full-duplex digital subscriber loop system is also studied.

Primary attention in this work is centered on techniques amenable to implementation in MOSLSI technology.

N-S Lin, D. A. Hodges, and D. G. Messerschmitt are with the Department of Electrical Engineering and Computer Sciences and the Electronics Research Laboratory, University of California, Berkeley, California 94720.
This research is supported by grants from Advanced Micro Devices, Fairchild Semiconductor, Harris Corp., National Semiconductor, and Racal-Vadic, with a matching grant from the University of California's MICRO program.

2. Introduction

The *Digital Subscriber Loops* (DSL) is one of the most important elements of the *Integrated Services Digital Network* (ISDN). It is to provide full duplex digital transmission over the conventional twisted pair at some desired data rate. One proposed data rate is 160Kb/s, where two pulse-code modulated (PCM) voice channels, each at 64Kb/s, and 32 Kb of other data are transmitted simultaneously.

The *Echo cancellation* or *hybrid mode* technique is one of the promising approaches of providing full-duplex digital transmission for digital subscriber loops. In this mode, a *hybrid transformer* is used to separate the transmitted and received signals. Because of the imperfection of impedance matching of the hybrid transformer, there will be some leakage of the near-end transmitted signal through the hybrid to the receiver. This is called near end echo signal. An echo canceller is therefore used to generate an estimate of the echo signal, or echo replica, so that it can be subtracted from the received signal to make a better estimate of the far end signal. Fig. 1 is the block diagram of the echo cancellation mode digital subscriber loop. The transmit and receive filters and equalizers are required for the purpose of equalizing the line phase nonlinearity and minimizing the intersymbol interference. In order to have 20 dB signal to noise ratio, more than 50 dB echo cancellation will be required if 40 dB attenuation is assumed for far end signal at the receiver.

3. Problem and Solution Formulation

Discrete-time techniques are considered to be more feasible than that of continuous-time in integrated-circuit implementation. Therefore, only discrete-time techniques are considered here. Fig. 2 is the block diagram of the subscriber end. The echo path can be modeled as a linear system with impulse response $g(k)$, the resultant sampled echo signal e_n will be the convolution of the near end input data X_n with the sampled impulse response of echo path, i.e.,

$$e_n = \sum_{k=0}^{N-1} g(k) X_{n-k}$$

One very important feature accompanied with the discretization is that only the sampled echo signal is important and it depends on the echo path impulse response at the sampling points only. Therefore, different sampling phases will give different echo signals. The linear echo canceller is an adaptive transversal filter. The output of the echo canceller, or echo replica, is:

$$\hat{e}_n = \sum_{k=0}^{M-1} c(k) X_{n-k}$$

where $c(k)$'s are the coefficients of echo canceller, and M is the number of coefficients. The coefficients are adapted by a feedback loop to match the values of the sampling points of echo path impulse response. If the number of coefficients is large enough and if the coefficients $c(k)$'s have been adapted to $g(k)$, the desired cancellation can be achieved.

3.1. Problem formulation

When jitter occurs, the output of the digital phase locked loop will have a discrete phase jump. The jump in phase will result in a different echo signal because of the change in $g(k)$'s. Since the coefficients of echo canceller can not adapt simultaneously to be equal to the new $g(k)$'s, the predicted echo signal, i.e., echo replica, will be different from the real echo. Therefore, the desired cancellation can not be achieved and the system performance degrades.

In order to reduce the degradation in performance in the presence of jitter (phase jump), the values of the echo path impulse response at new sampling phases have to be obtained. In other words, the new coefficients for the echo canceller have to be calculated when jitter occurs. This can be achieved by first reconstructing the continuous waveform of the echo path impulse response and then calculating the new sample values according to the magnitude of the phase jump. The data available for reconstructing the continuous waveform is the echo canceller coefficients, which are equal to the values of the echo path impulse response at previous sampling phase spaced from one another by one sampling period.

Two major difficulties have to be overcome before this technique is applicable.

The first difficulty is the aliasing distortion due to *baud-rate sampling*. Echo canceller is the most complex portion of digital subscriber loops. Its hardware complexity increases linearly with sampling rate due to the discrete-time nature of the system. Therefore, minimum sampling rate is desirable. Baud rate is the lower limit of the sampling rate for a digital data transmission system and baud-rate sampling [1] has been shown to be a feasible technique. Therefore, our design is aimed at baud-rate sampling. But because of the baud-rate sampling, the data available for reconstructing the continuous waveform of echo path impulse response is not enough according to Nyquist theorem. There will be aliasing distortion introduced in the process of reconstructing the continuous waveform. In other words, the calculated sample values won't be equal to the real ones, and, as a result, there will be errors in predicting the new echo signal. Fig. 3 is the frequency response of echo signal before sampling. The power at frequencies higher than half baud rate will contribute to aliasing distortion.

The second problem is the distortion introduced by non-ideal low pass filtering. A low pass filter is needed in order to reconstruct continuous waveform from discrete sampled data. It is not desirable to requre a high order filter on a VLSI chip to perform the function of low pass filtering. The technique studied in this paper is *interpolation*. This is discussed in detail in section 3.4.

3.2. Partial Response Coding (PRC)

The proposed solution for the first problem is to shape the echo signal spectrum by using partial response coding (PRC), which is also known as correlative-level coding [2][3][4][5].

The basic idea of PRC is to combine successive binary bits together by some given rules. It introduces intersymbol interference in a controlled way. As a result, the autocorrelation of the input sequence is changed accordingly. There are several advantages associated with PRC. Among them, it can provide desirable spectrum shaping as well as

increase the bit rate that can be transmitted over a given channel. According to the generating mechanism of PRC, it can be grouped into five classes [3], namely:

class I: Equal amplitude superposition,

class II: Triangular envelope superposition,

class III: Superposition including negative components,

class IV & V: Superpositions free of DC transmission.

In addition to the goal of reducing the echo signal power at frequencies higher than half baud rate, some aspects [6] of the characteristics of the transmission media and the equipment of the DSL system also have to be considered in chosing the partial response code because the use of PRC will affect the spectrum of the far end signal as well. They are:

1. No DC transmission through hybrid transformers.
2. Equalization is difficult at low frequencies.
3. Large attenuation at very high frequencies (attenuation proportional to square root of transmission frequency).
4. Crosstalk between neighboring pairs increases dramatically at high frequencies.

One partial response code which satisfies the criteria mentioned above is the *modified duobinary code* (class IV, n=3). It has spectral zeros at DC and half baud rate ($1/2\ f_b$). Fig. 4 is the block diagram of this scheme where D represents one data period delay. The output sequence is equal to the input sequence subtracted by its two-period-delayed version. The transfer function of this scheme is:

$$H(\omega) = 1-e^{-2j\omega T} = 2je^{-j\omega T}\sin(\omega T)$$

The magnitude of the transfer function is:

$$|H(\omega)| = 2|\sin(\omega T)|$$

This is plotted in Fig. 5.

If the modified duobinary PRC is introduced into the echo path, the resultant power spectrum of echo signal will be the original power spectrum multiplied by the square of the magnitude of the transfer function given above. By introducing the modified duobinary PRC, the power in the range of frequencies between half and one baud rate is reduced by 3.74 dB compared with that of alternate mark inversion (AMI) code, assuming the same total signal power. As a result, the aliasing distortion is reduced.

One other advantage associated with the use of modified duobinary PRC is that the error signal power due to jitter is reduced. This can be explained by examining the power spectrum of the error signal:

$$S_{error}(\omega) = 2\pi E[\alpha_n{}^2] S_{sequence}(\omega)\omega^2 |G(\omega)|^2$$

where α_n is the jitter at time n, $S_{sequence}(\omega)$ is the power spectrum of input data sequence and $G(\omega)$ is the transfer function of the filters in the echo path. Because of the ω^2 factor, the error power increases dramatically at high frequencies. The use of modified duobinary PRC reduces the high frequency component, which is also the original reason for using the PRC to reduce the aliasing distortion, and consequently, the error caused by jitter is reduced. The amount of improvement is 2.1 dB over AMI code.

3.3. Coder Implementation

There are some alternatives in realizing the modified duobinary code together with transmit and receive filters. They are shown in Fig. 6.

In the first scheme (MDB1), the coding operation is performed in the digital domain. The transmit and receive filters can be a raised-cosine filter (or any filter designed for minimizing intersymbol interference). The resultant frequency response is a sinusoid, which accounts for the modified duobinary code, multiplied by the response of the raised-cosine filter.

The second scheme (MDB2) is to perform the function of coder in the analog domain. In this case, the product of the response of the transmit filter and the receive filter is to equal the response of modified duobinary code multiplied by that of a low pass filter

whose cutoff frequency is $0.5f_b$. In other words, its magnitude response is

$$|Tx(f)Rec(f)| = \begin{cases} 2|\sin(2\pi fT)| & -0.5f_b \leq f \leq 0.5f_b \\ 0 & elsewhere \end{cases}$$

The third scheme (MDB3) lies between the two methods mentioned above. It factorizes the modified duobinary code $1-e^{-2j\omega T}$ into $(1-e^{-j\omega T})(1+e^{-j\omega T})$ and realizes the first part in digital domain and the second part by using analog transmit and receive filters. Notice that $(1+e^{-j\omega T})$ is the ordinary duobinary code and is easy to implement in hardware.

These different schemes are compared in section 4.

3.4. Interpolation

Mathematically, a k-th order interpolation is to fit k+1 points by a k-th order polynomial. For example, first order interpolation is to use a straight line to fit two given points and second order interpolation is to fit three given points by a parabola. In general, the k-th order polynomial which fits k+1 points is given by:

$$f(t) = f_n + (t-t_n)\frac{\nabla f_n}{h} + (t-t_n)(t-t_{n-1})\frac{\nabla^2 f_n}{2}h^2$$
$$+ \cdots + (t-t_n)\cdots(t-t_{n-k+1})\frac{\nabla^k f_n}{k!\,h^k}$$

where

$$\nabla f_n = f_n - f_{n-1}$$
$$\nabla^2 f_n = \nabla(f_n - f_{n-1})$$
$$= f_n - 2f_{n-1} + f_{n-2}$$
$$h = t_n - t_{n-1}$$

and f_n is the value of the function at t=n.

Instead of a low pass filter, an interpolator is used here to perform the function of low pass filtering, i.e., to reconstruct the continuous waveform from discrete sampled data. There is a tradeoff between computation accuracy and hardware complexity. The higher the order of interpolation is, the better the approximation to ideal low pass filter will be.

But in the meantime, the hardware will become more complicated. Therefore, minimum order of interpolation is desired in order to minimize the hardware complexity, yet still adequate to achieve the desired accuracy. Based on computer simulation, the minimum order of interpolation acceptable is found to be two. Some computer simulation results are presented in section 5.

4. Crosstalk Interference

Crosstalk is one of the most significant limitations in DSL. There are two types of crosstalk, *near-end crosstalk* (NEXT) and *far-end crosstalk* (FEXT) [7][8]. These are shown in Fig. 7. Much study has been done and the results are that NEXT increases at a rate of 4.5 dB/octave ($f^{3/2}$) while FEXT increases by 6 dB/octave (f^2). Since signals flow in two directions simultaneously in DSL, NEXT is the dominant crosstalk interference. Before analyzing the NEXT power, first we define the power transfer function X_{next} :

$$|X_{next}|^2 = K\left(\frac{f}{f_b}\right)^{\frac{3}{2}}$$

where K is an empirical constant. The power transfer function accounts for the mechanism of the coupling between twisted pairs.

In this analysis, the signal path is modeled as shown in Fig. 8 where $C(f)$ is the transfer function of the channel and $1/C(f)$ is the equalizer which equalizes the channel response, and

$$|C(f)|^2 = \exp(-\alpha_o\sqrt{f})$$

The crosstalk power is given by:

$$P_{next} = \int_0^{f_b} K_1 S_x(f)|X_{next}(f)|^2 \frac{1}{|C(f)|^2} df$$

and $S_x(f)$ is the signal power spectrum:

$$S_x(f) = S_{sequence}(f)\frac{|G(f)|^2}{T}$$

where $S_{sequence}(f)$ is the power spectrum of input binary data sequence, $G(f)$ is the

response of transmit and receive filters, and T the duration of one baud period.

One general assumption is made here for analysis:

The input data sequence $\{ X_n \}$ is random with the probability of X_n being 0 and 1 equal to 0.5 respectively.

The signal power spectrum $S_x(f)$ of binary code and AMI code are:

$$S_{x_{bi}} = \frac{|G(f)|^2}{T}$$

$$S_{x_{AMI}} = \frac{|G(f)|^2}{T}\sin^2\pi f T$$

for $-f_b \leqslant f \leqslant f_b$. If the transmit and receive filters are assumed to be raised-cosine filter with 100 percent excess bandwidth, $G(f)$ will be equal to $\cos^2((\pi f)/(2f_b))$ for $-f_b \leqslant f \leqslant f_b$, and 0 elsewhere.

The signal power spectrum of modified duobinary code of different schemes are:

$$S_{x_{MDB\,1}} = \frac{1}{T}\cos^4(\frac{\pi f}{2f_b})\sin^2(\frac{2\pi f}{f_b}) \quad -f_b \leqslant f \leqslant f_b$$

for the raised-cosine transmit and receive filters, and

$$S_{x_{MDB\,2,3}} = K_2\frac{1}{T}\sin^2(\frac{2\pi f}{f_b}) \quad -0.5f_b \leqslant f \leqslant 0.5f_b$$

K_2 is the normalization constant:

$$K_2 = \frac{\int_0^{f_b}\cos^4(\frac{\pi f}{2f_b})df}{\int_0^{f_b}df}$$

Based on the above equations, the NEXT power of different codes are compared by the NEXT power per unit received signal power. The results are summarized in Table 1. Here AMI code is used as reference and normalized to 0 dB.

Since the binary code does not give zero at DC, it makes sense to compare the binary code with a self-equalized pulse shape. Here the Wal-2 code is used for comparison. The result is also shown in Table 1. From Table 1, modified duobinary codes give smaller

Code	$\frac{\frac{P_{next}}{P_S}}{(\frac{P_{next}}{P_S})_{AMI}}$
AMI	0dB
MDB1	-2.84dB
MDB2,3	-3.57dB
Binary	-2.68dB
$Binary_{Wall}$	2.61dB

Table 1.

NEXT interference than any of the other codes.

Although MDB2 and MDB3 have smaller NEXT interference than MDB1 , there are some disadvantages associated with MDB2,3 compared with MDB1. They are:

(1) More complicated hardware for transmit and receive filters.

(2) Number of coefficients of echo canceller is larger because of longer impulse response.

The second disadvantage is due to the fact that the impulse response falls off as t^{-1} for MDB2,3 while t^{-3} for MDB1 (for raised-cosine with 100 percent excess bandwidth). Fig. 9 shows the power spectrum and impulse response of various coding schemes.

5. Simulation Results

The transmit and receive filters used in the simulation are designed to minimize the intersymbol interference. They have a single real pole and two pairs of complex poles respectively [8]. The first part of the simulation assumes that the transmitter does not follow the recovered timing phase. This serves the purpose of understanding the characteristics of the jitter performance, which includes the degree of degradation and the rate of convergence.

Fig. 10 shows the jitter performance of the system with AMI code. The magnitude of jitter is 1/ 64. Here, the system is assumed to be purely linear, and therefore, the echo canceller is an adaptive transversal filter with linear taps only. Three curves are shown in the figure. They represent the situation of no interpolation, first order interpolation, and

second order interpolation respectively. In this figure, the result of first order interpolation is seen to be worse than that of no interpolation. This is because the improvement due to interpolation is less significant than the distortion introduced by non-ideal low pass filtering, which is first order interpolation. The result of using second order interpolation does improve the system performance, but the improvement is less than 3 dB.

Fig. 11 shows the jitter performance of a linear system, but with modified duobinary PRC instead. Again three curves are shown in this figure. They correspond to those curves shown in Fig. 10. The result is that, for a system with modified duobinary PRC, the use of second order interpolation improves the performance by more than 7 dB. If compared to an AMI system, more than 10 dB improvement is achieved. Fig. 12 is the jitter performance of periodic jitter. The magnitude of jitter is 1/ 512 per step.

Fig. 13 is the jitter performance of a slightly nonlinear system. Here, the echo canceller is assumed to have four additional nonlinear taps [9]. The result indicates that this technique also works for slightly nonlinear systems.

If the transmitter follows the recovered timing phase, the effect of jitter will only last for a very short period of time. The number of periods it lasts depends on how fast the impulse response dies away. Typically, it is smaller than twenty periods. The second part of the simulation assumes that the transmitter phase is synchronized to the recovered timing phase. Since every point in those figures of the first part simulation has been calculated by averaging over one thousand periods, it is not possible to see the effect of jitter for the scheme of the second part. But still, transient response should be examined. Since the transient response of jitter performance depends on the input data pattern, the simulations and calculations are done by examining the worst situation and root-mean-square case. The results are shown in Fig. 14. They once again confirm that the use of modified duobinary PRC and second order interpolation improves the jitter performance.

6. Conclusions

The approach of using modified duobinary PRC and second order interpolation to improve jitter performance is described in this paper. The effect of modified duobinary PRC on crosstalk interference is also studied. Computer simulations are presented.

7. Acknowledgement

Many thanks are due to Jeremy Tzeng for his helpful discussion and advice. The discussion with Graham Brand on crosstalk is also appreciated.

REFERENCES

[1] C-P Jeremy Tzeng, D. A. Hodges, and D. G. Messerschmitt, "Timing Recovery In Digital Subscriber Loops Using Baudrate Sampling," to be presented at ICC 85.

[2] Adam Lender, "Correlative Level Coding for Binary-Data Transmission," *IEEE Spectrum February 1966, pp. 104-115*

[3] E.R. Kretzmer, "Binary Data Communication by Partial Response Transmission," *Conf. Rec. 1965 IEEE Ann. Communications Conv., pp. 451-455.*

[4] P. Kabal and S. Pasupathy, "Partial-Response Signaling," *IEEE Transactions on Communications*, Vol. com-23, No. 9, Sep. 1975, pp. 921-934.

[5] Mischa Schwartz, "Information Transmission, Modulation, and Noise," Third Edition, McGraw-Hill, 1980

[6] Frank F. E. Owen, "PCM and Digital Transmission Systems" McGraw-Hill, 1982

[7] B. R. Narayana Murthy, "Crosstalk Loss Requirements for PCM Transmission," *IEEE Transactions on Communications*, VOL. COM-24, No.1, Jan. 1976.

[8] G. H. Brand and D. G. Messerschmitt, "Multilevel Coding for the Digital Subscriber Loop," in preparation.

[9] O. Agazzi, D. G. Messerschmitt, and D. A. Hodges, "Nonlinear Echo Cancellation of Data Signals," *IEEE Transactions on Communications*, Vol. COM-30, Nov. 1982, pp. 2421-2433.

Figure Captions

Figure 1. Echo Cancellation mode Digital Subscriber Loop

Figure 2. Block Diagram of Subscriber End

Figure 3. Frequency Response of Echo Path

Figure 4. Block Diagram of Modified Duobinary Coder

Figure 5. Transfer Function of Modified Duobinary PRC

Figure 6(a). Modified Duobinary I Coder

Figure 6(b). Modified Duobinary II Coder

Figure 6(c). Modified Duobinary III Coder

Figure 7. Near-End Crosstalk and Far-End Crosstalk

Figure 8. Model for NEXT Analysis

Figure 9(a). Power Spectrum and Impulse Response of Binary Code.

Figure 9(b). Power Spectrum and Impulse Response of MDB1 PRC.

Figure 9(c). Power Spectrum and Impulse Response of MDB2,3 PRC.

Figure 10. Jitter Performance (AMI Code)

Figure 11. Jitter Performance (Modified Duobinary PRC)

Figure 12(a). Jitter Performance of Periodic Jitter

Figure 12(b). Jitter Performance of Periodic Jitter

Figure 12(c). Jitter Performance of Periodic Jitter

Figure 12(d). Jitter Performance of Periodic Jitter

Figure 13(a). Jitter Performance of Nonlinear System (Modified Binary PRC, No Interpolation)

Figure 13(b). Jitter Performance of Nonlinear System (Modified Binary PRC, 2nd Order Interpolation)

Figure 14(a). Jitter Performance, Transient Response (AMI, rms)

Figure 14(b). Jitter Performance, Transient Response (AMI, worst case)

Figure 14(c). Jitter Performance, Transient Response (Modified Duobinary PRC, rms)

Figure 14(d). Jitter Performance, Transient Response (Modified Duobinary PRC,

worst case)

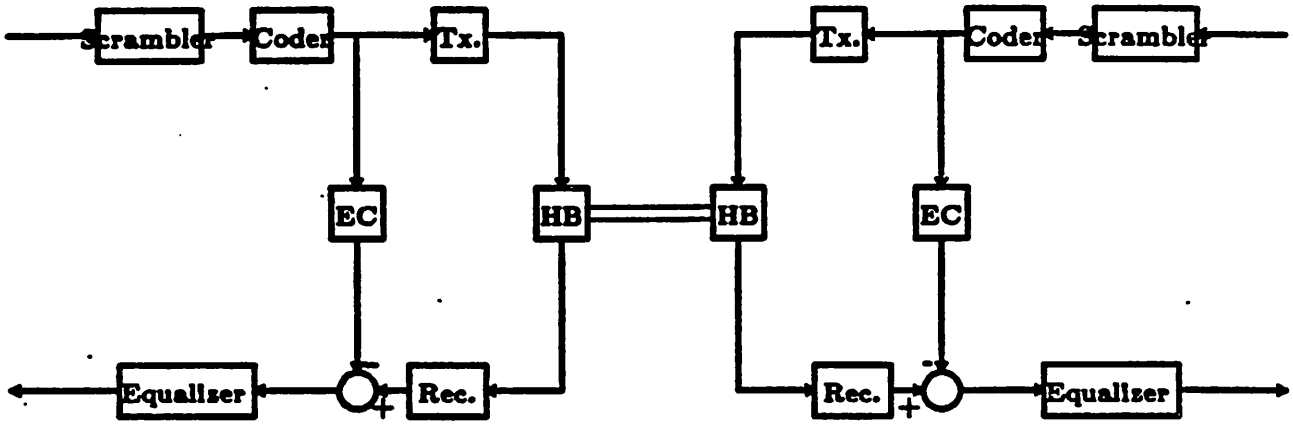

Figure 1. Echo Cancellation mode Digital Subscriber Loop

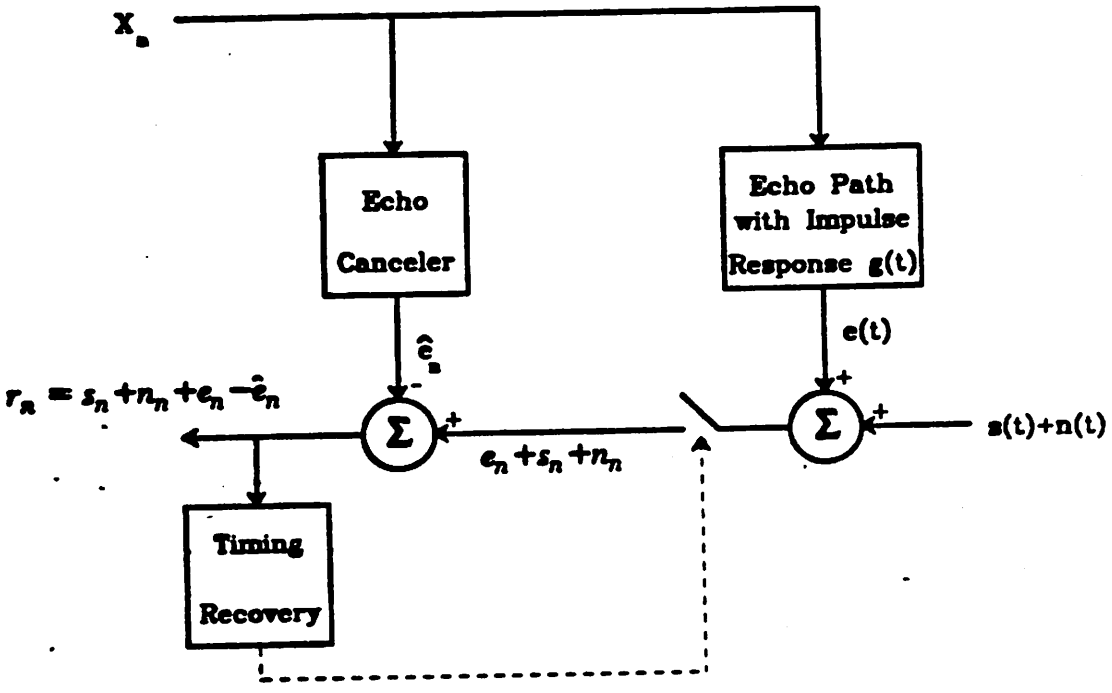

Figure 2. Block Diagram of Subscriber End

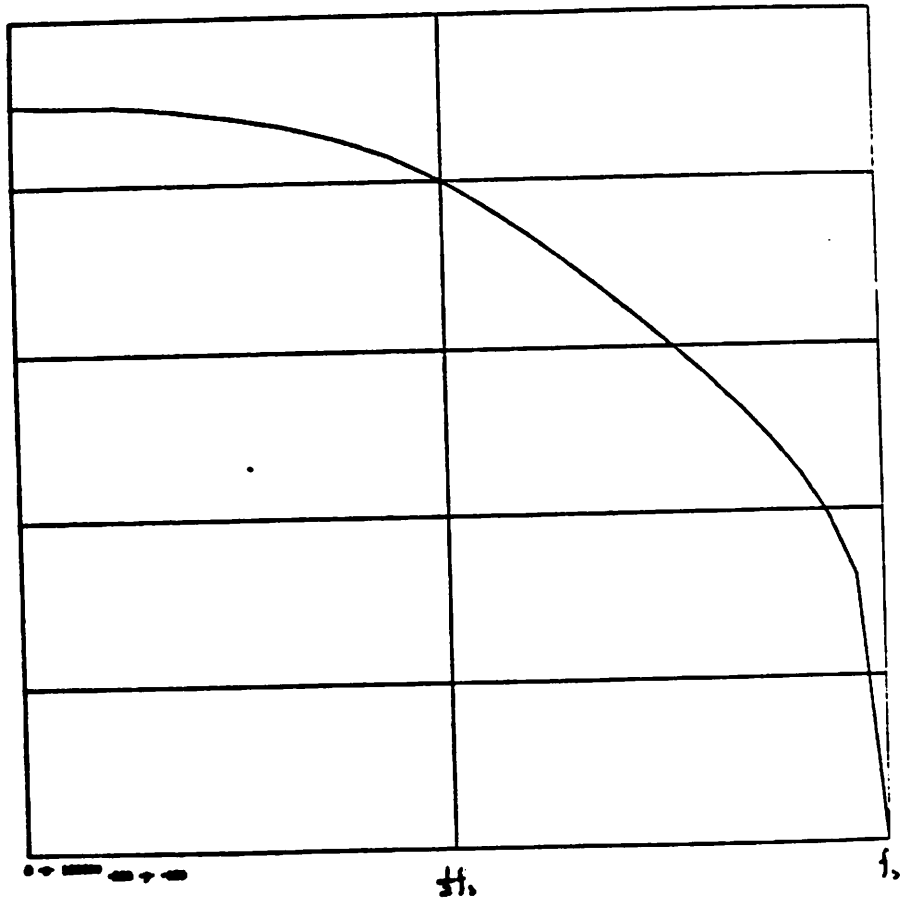

Figure 3. Frequency Response of Echo Path

(without partial response coding)

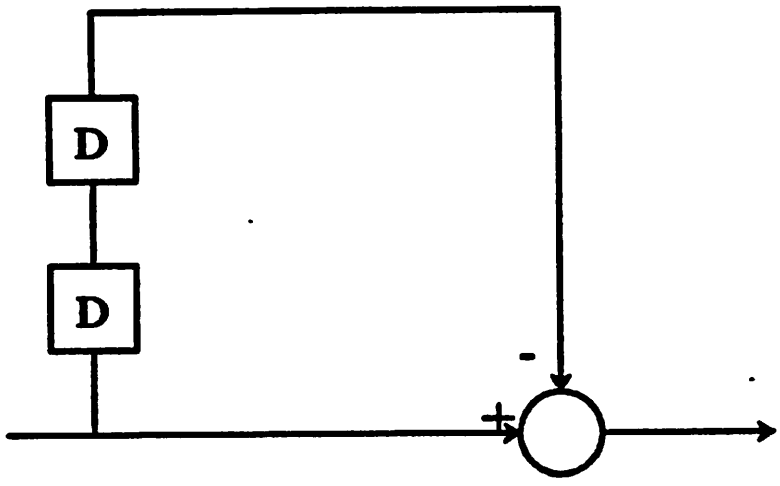

Figure 4. Block Diagram of Modified Duobinary Coder

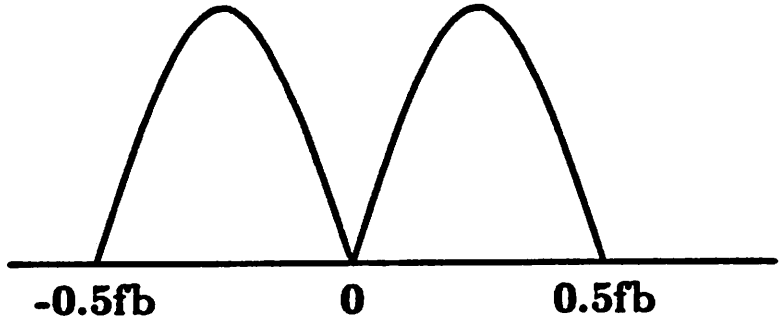

Figure 5. Transfer Function of Modified Duobinary PRC

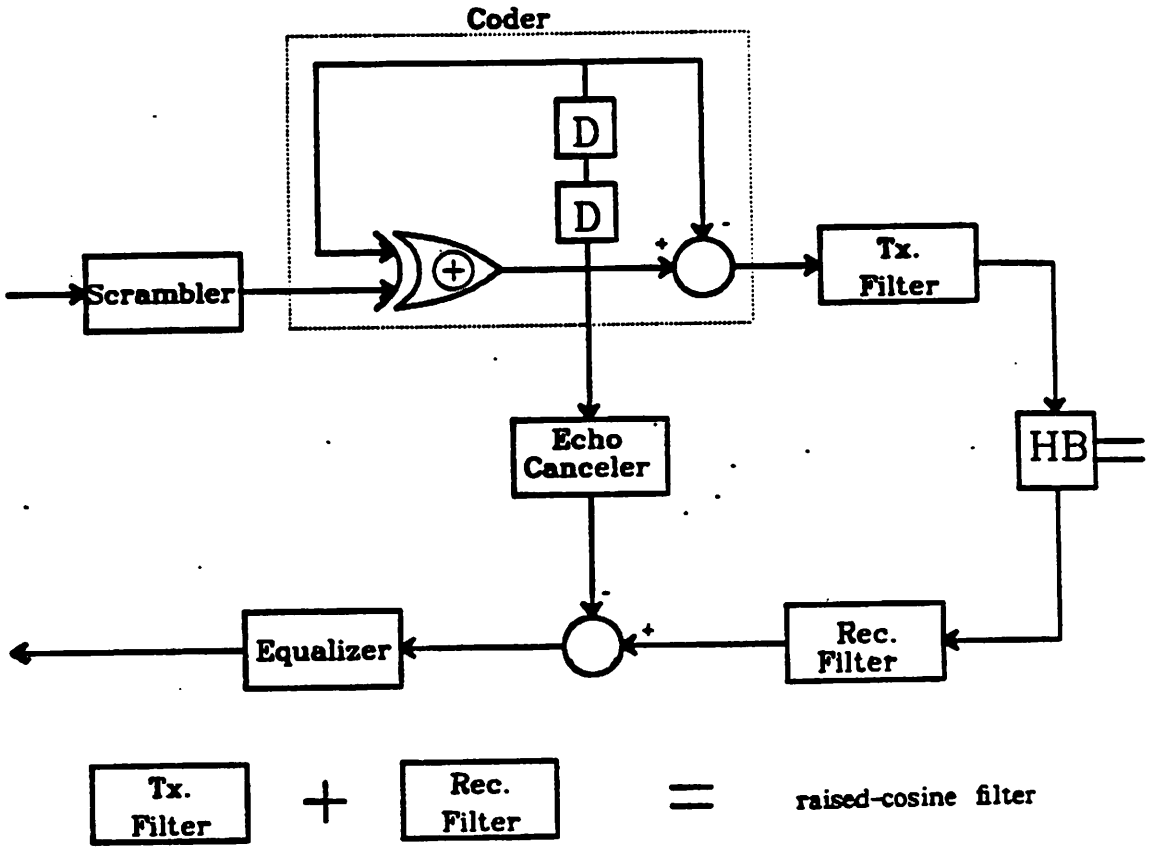

Figure 6(a). Modified Duobinary I Coder

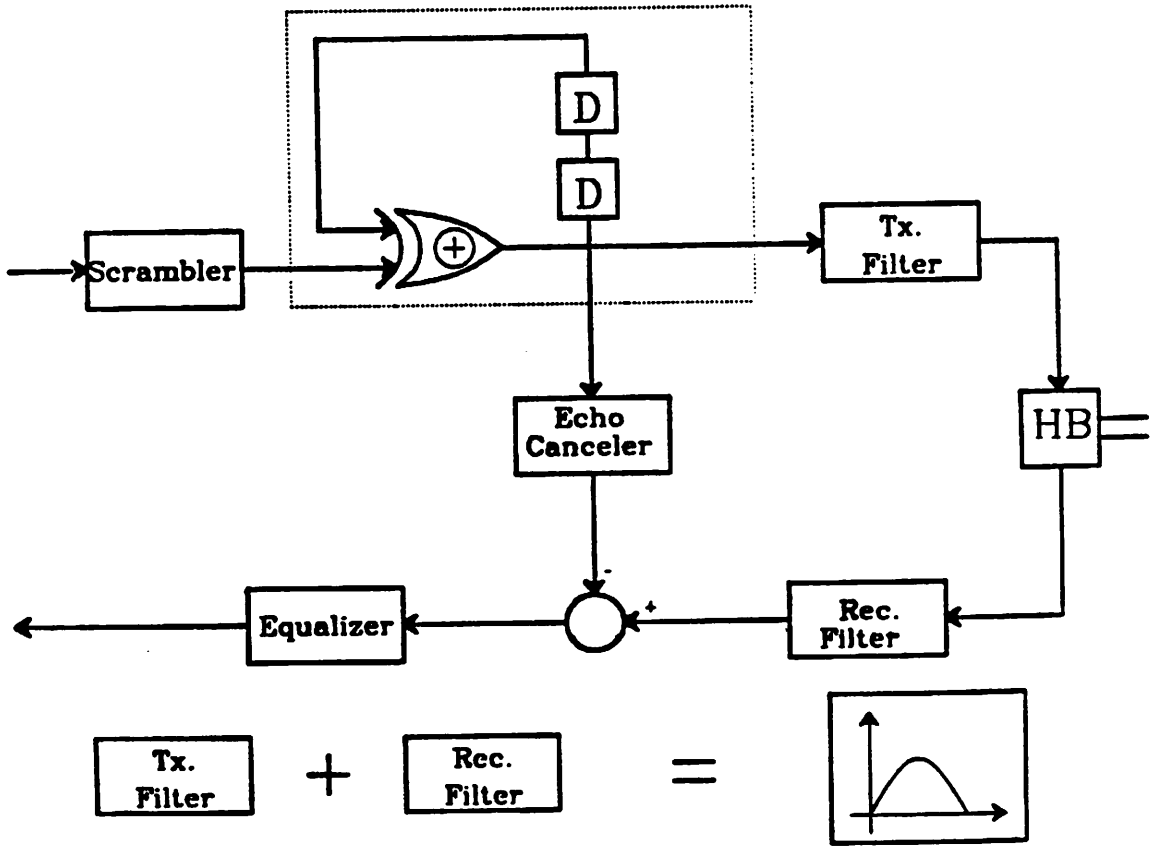

Figure 6(b). Modified Duobinary II Coder

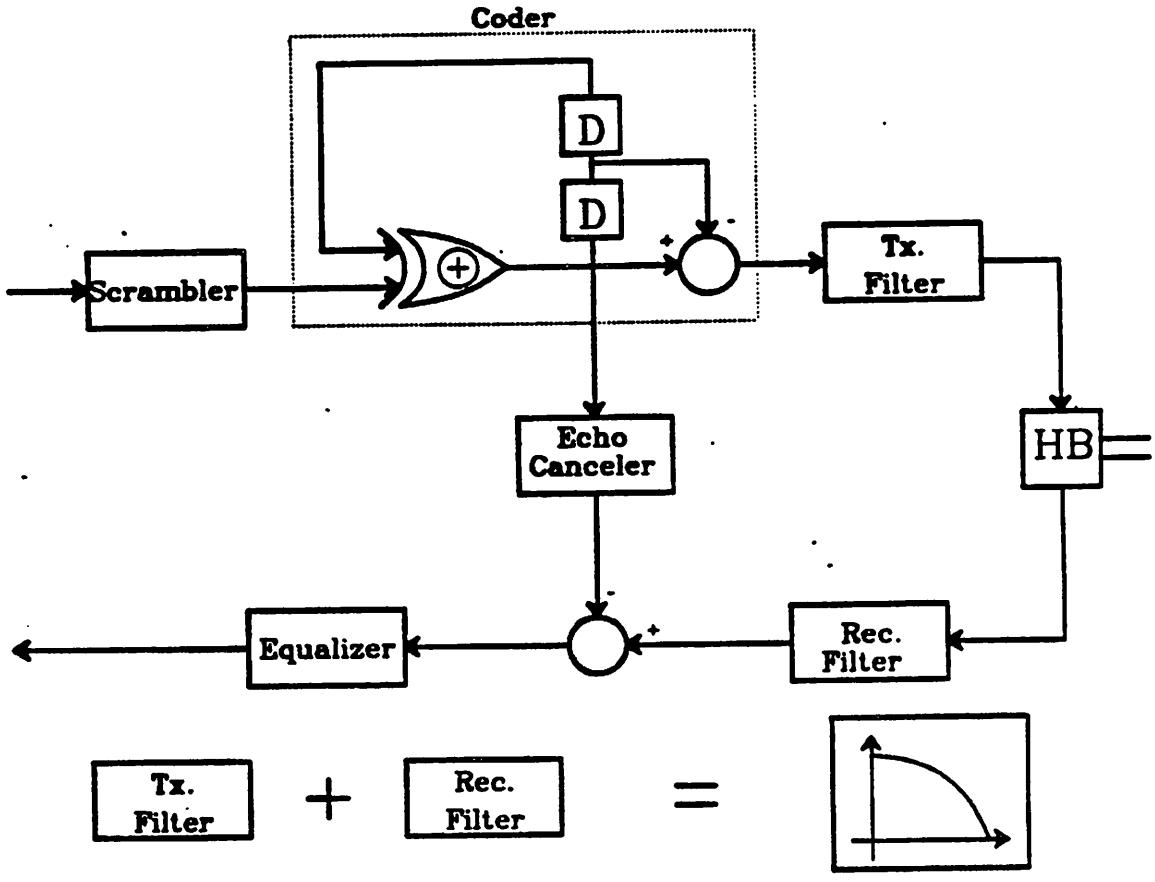

Figure 6(c). Modified Duobinary III Coder

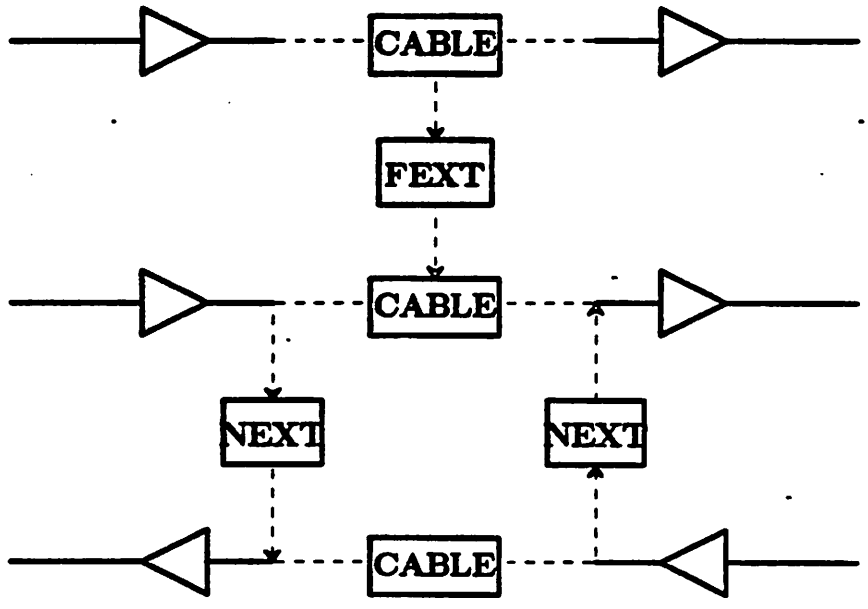

Figure 7. Near-End Crosstalk and Far-End Crosstalk

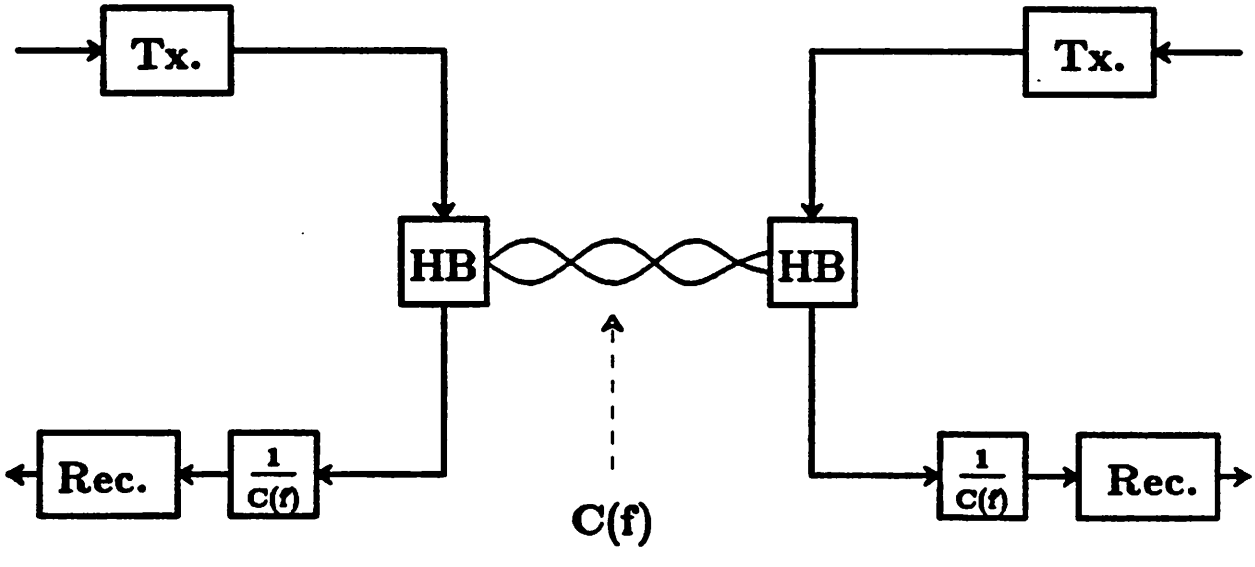

Figure 8. Model for NEXT Analysis

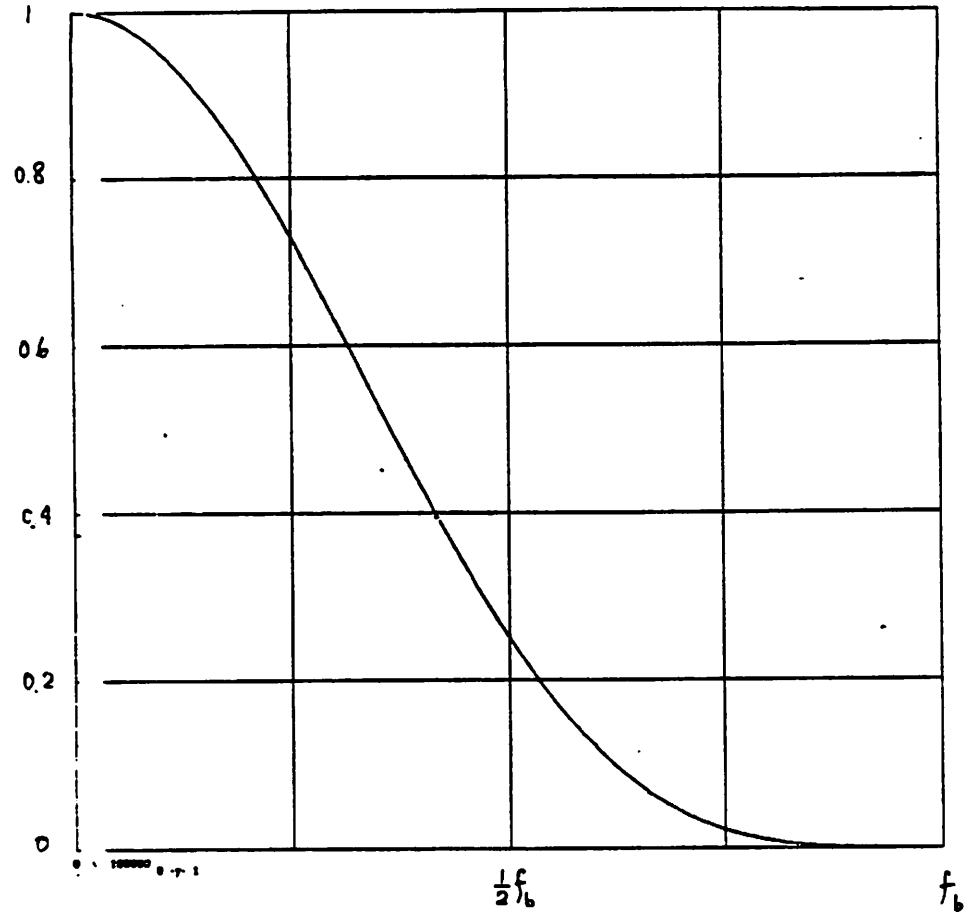

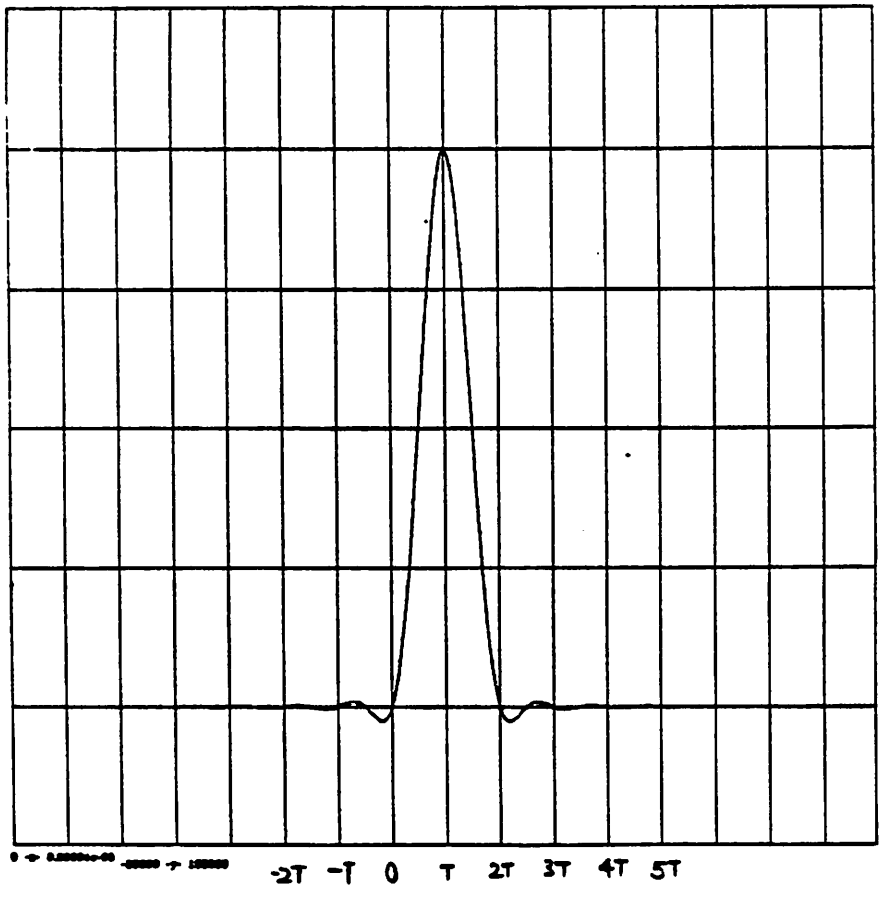

Figure 9(a). Power Spectrum and Impulse Response of Binary Code.

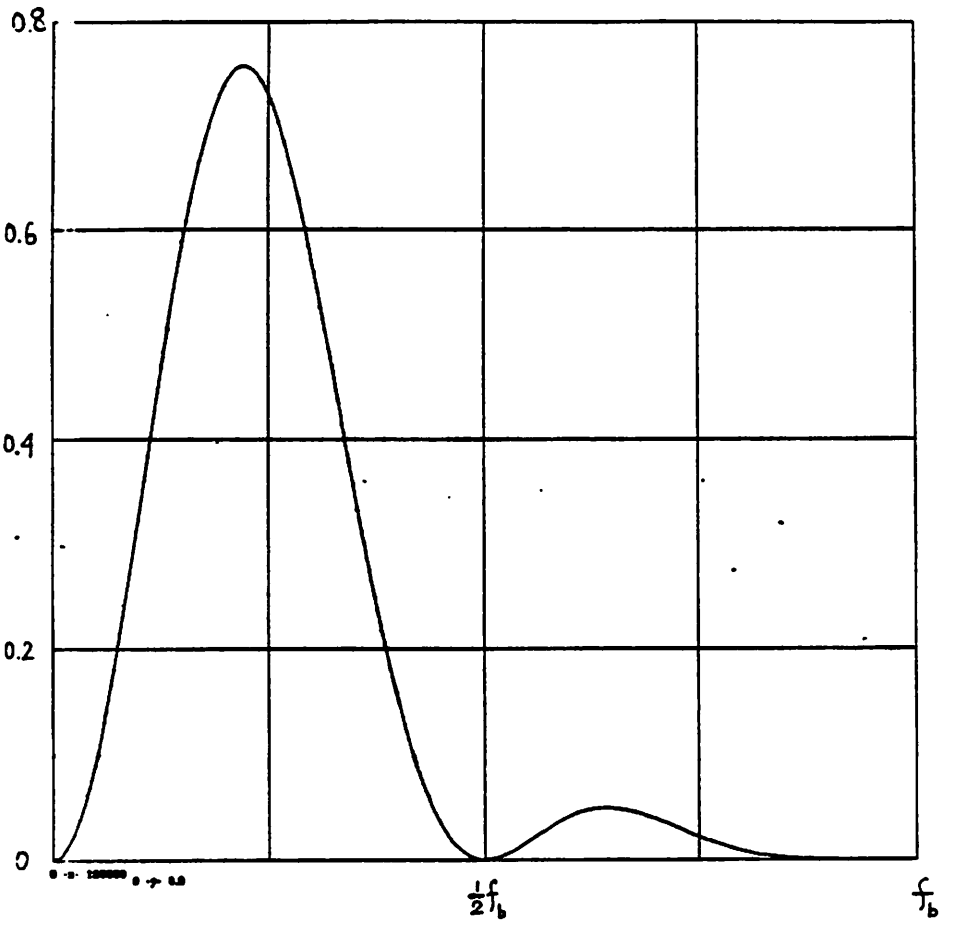

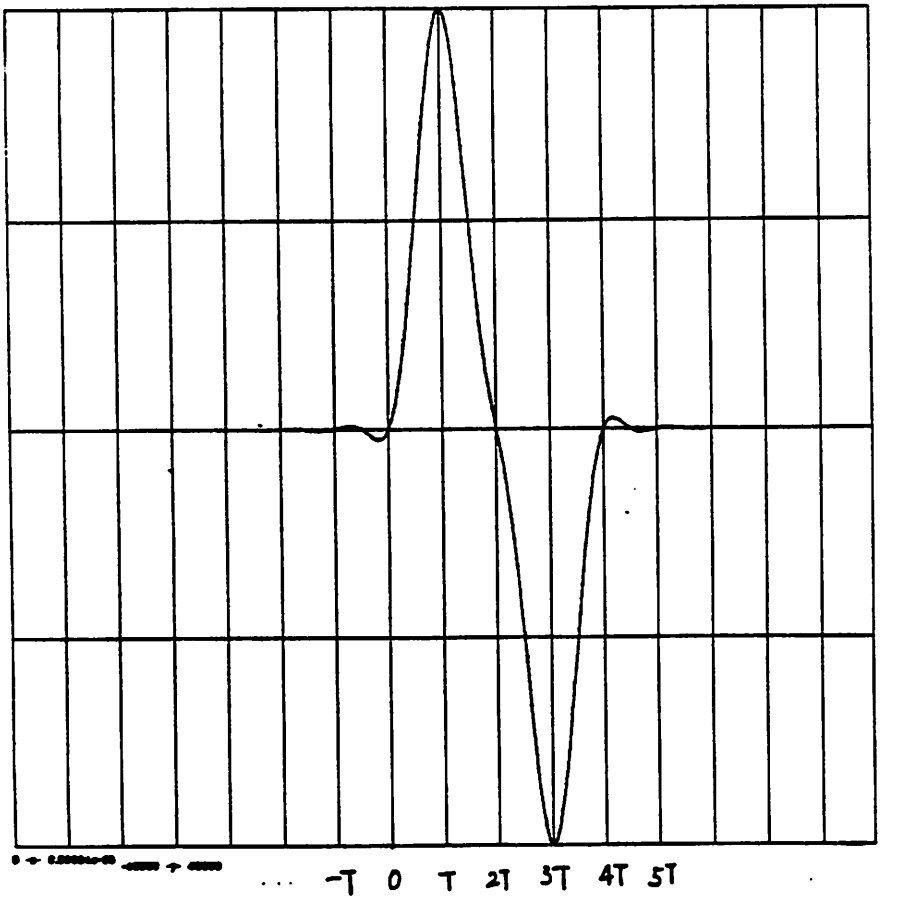

Figure 9(b). Power Spectrum and Impulse Response of MDB1 PRC.

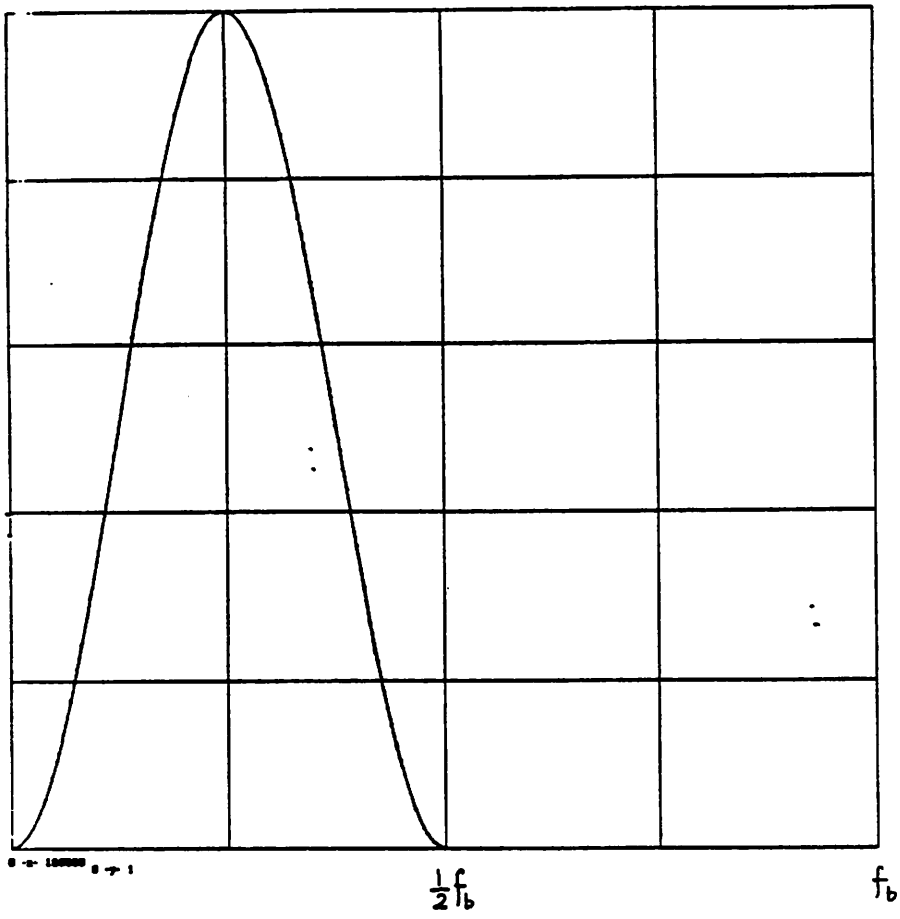

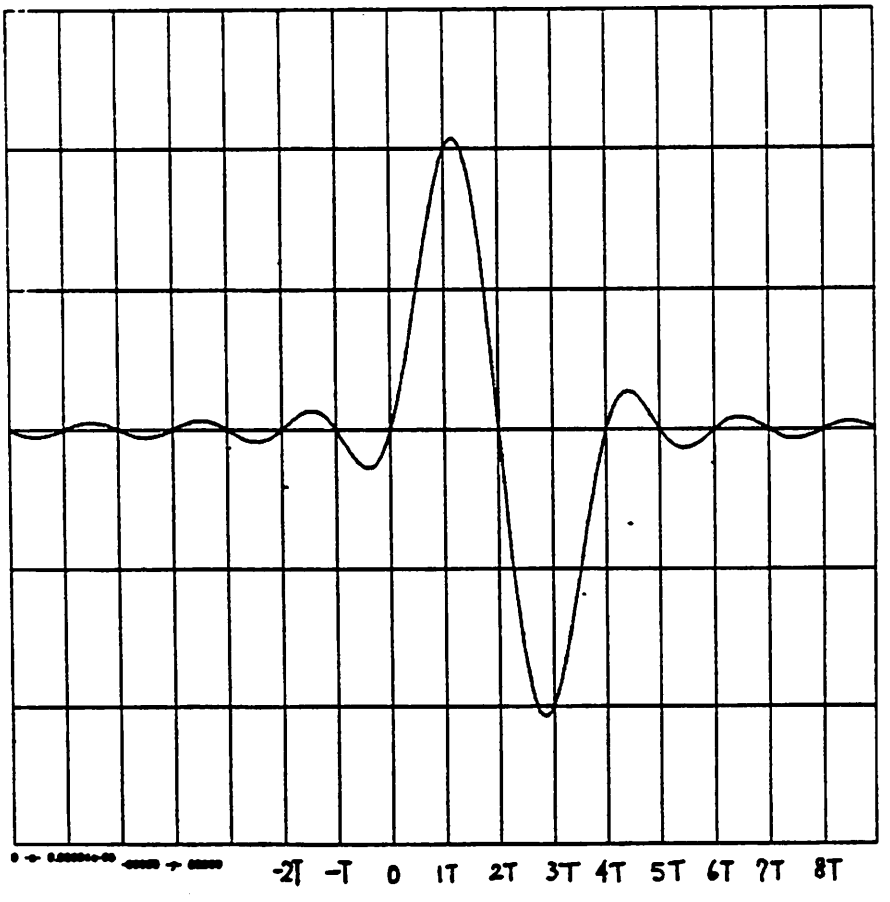

Figure 9(c). Power Spectrum and Impulse Response of MDB2.3 PRC.

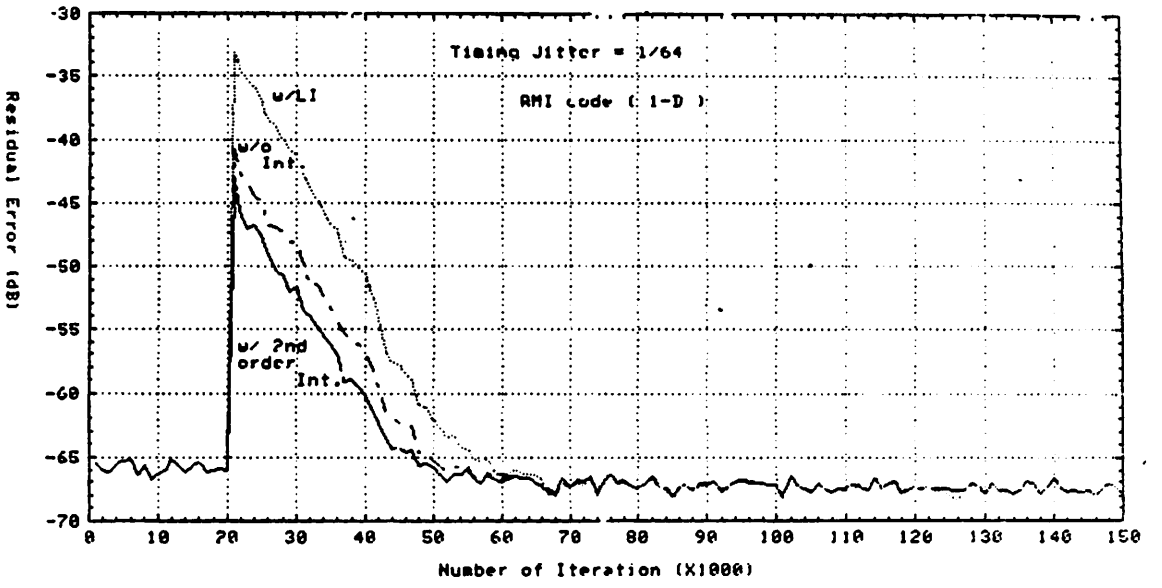

Figure 10. Jitter Performance (AMI Code)

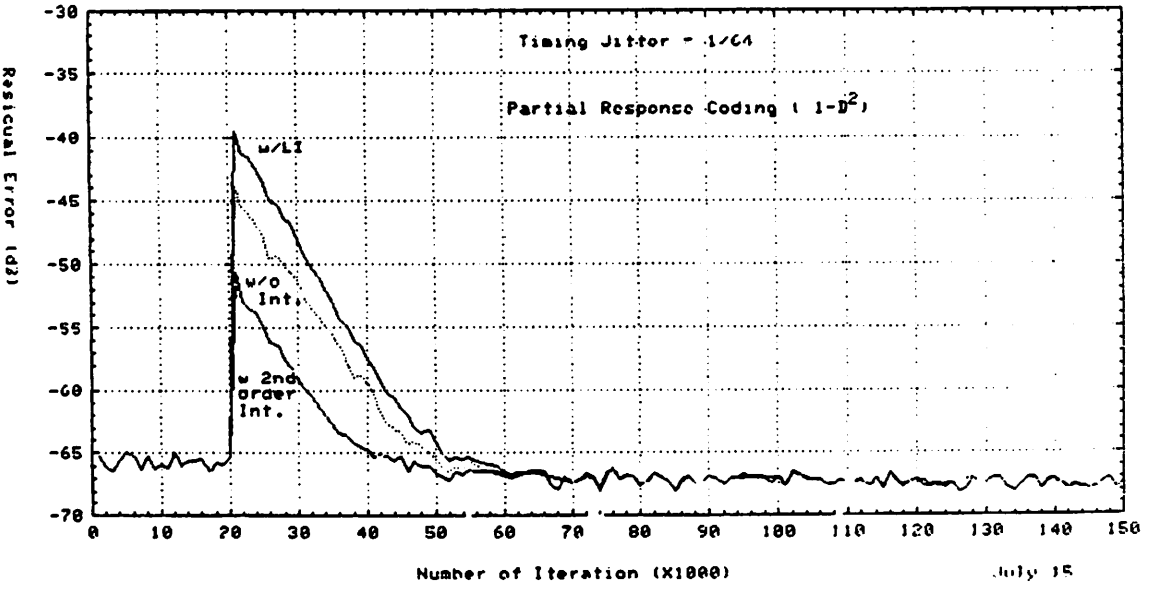

Figure 11. Jitter Performance (Modified Duobinary PRC)

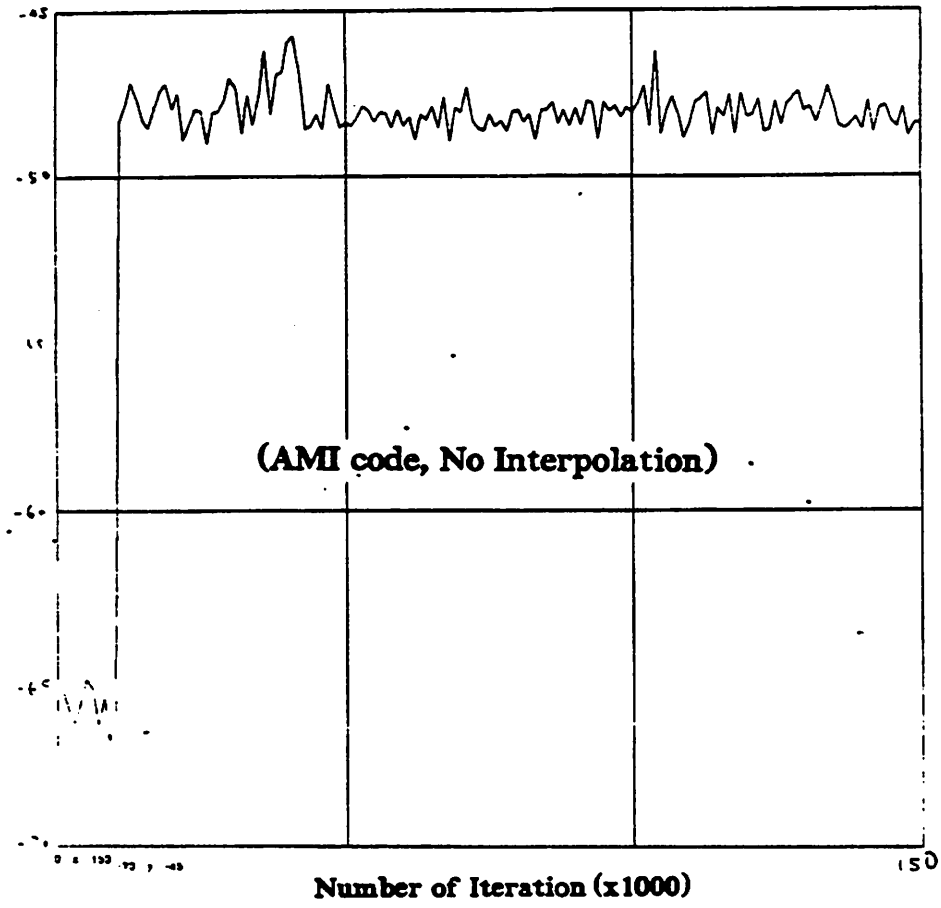

Figure 12(a). Jitter Performance of Periodic Jitter

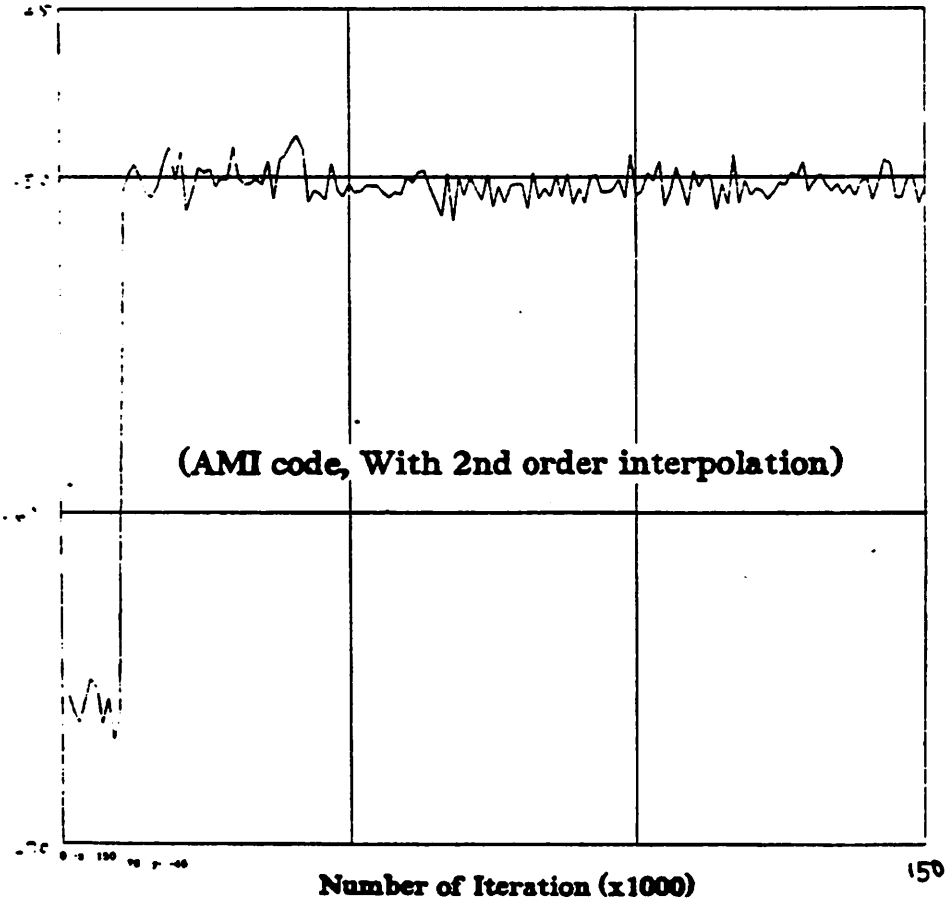

Figure 12(b). Jitter Performance of Periodic Jitter

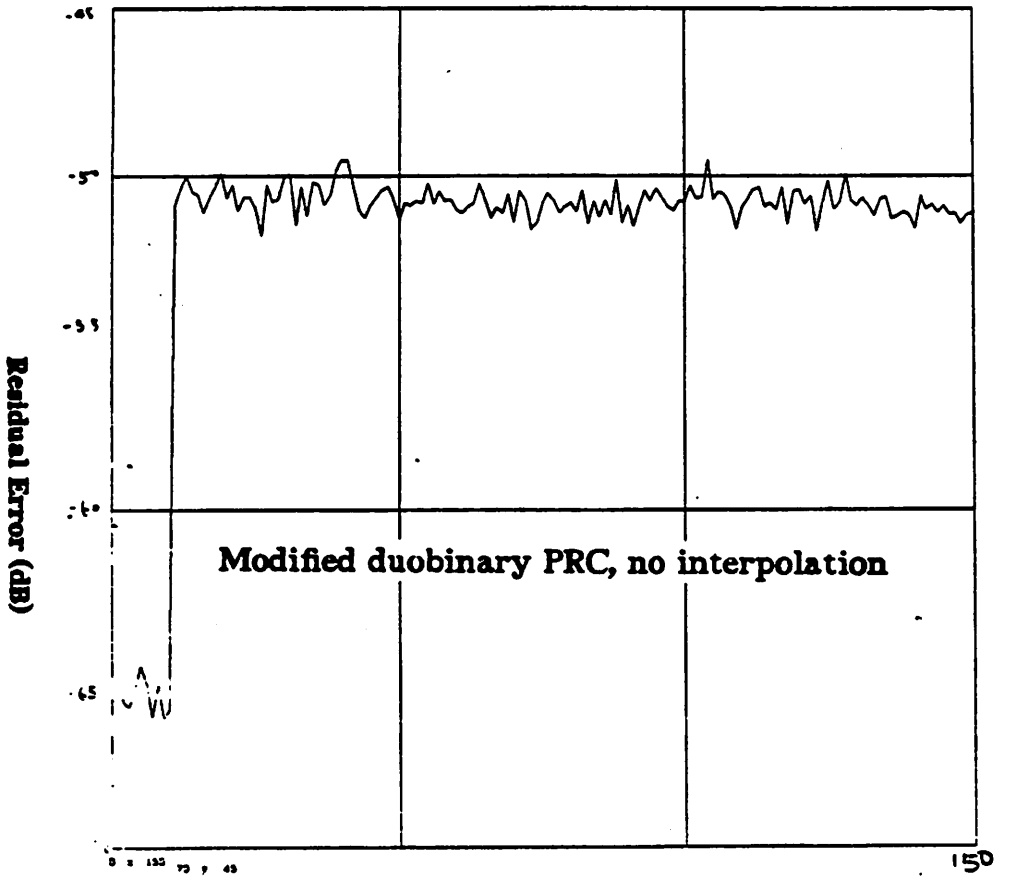

Figure 12(c). Jitter Performance of Periodic Jitter

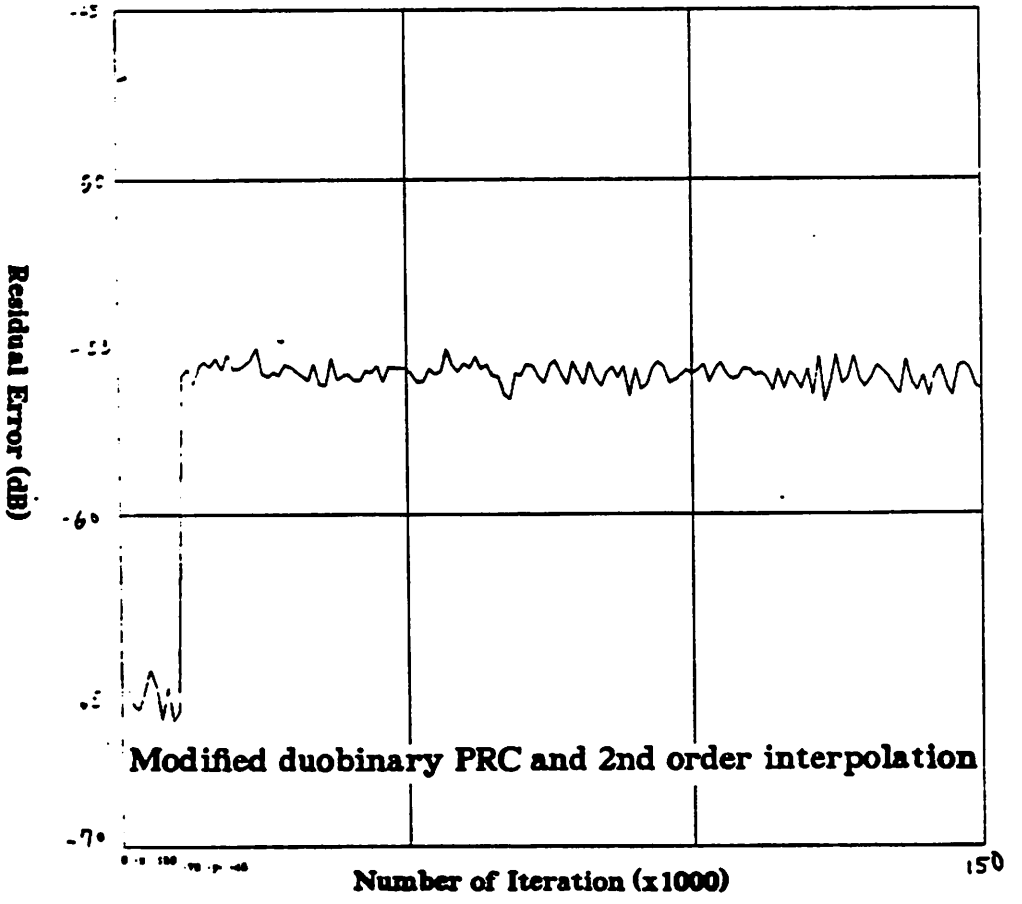

Figure 12(d). Jitter Performance of Periodic Jitter

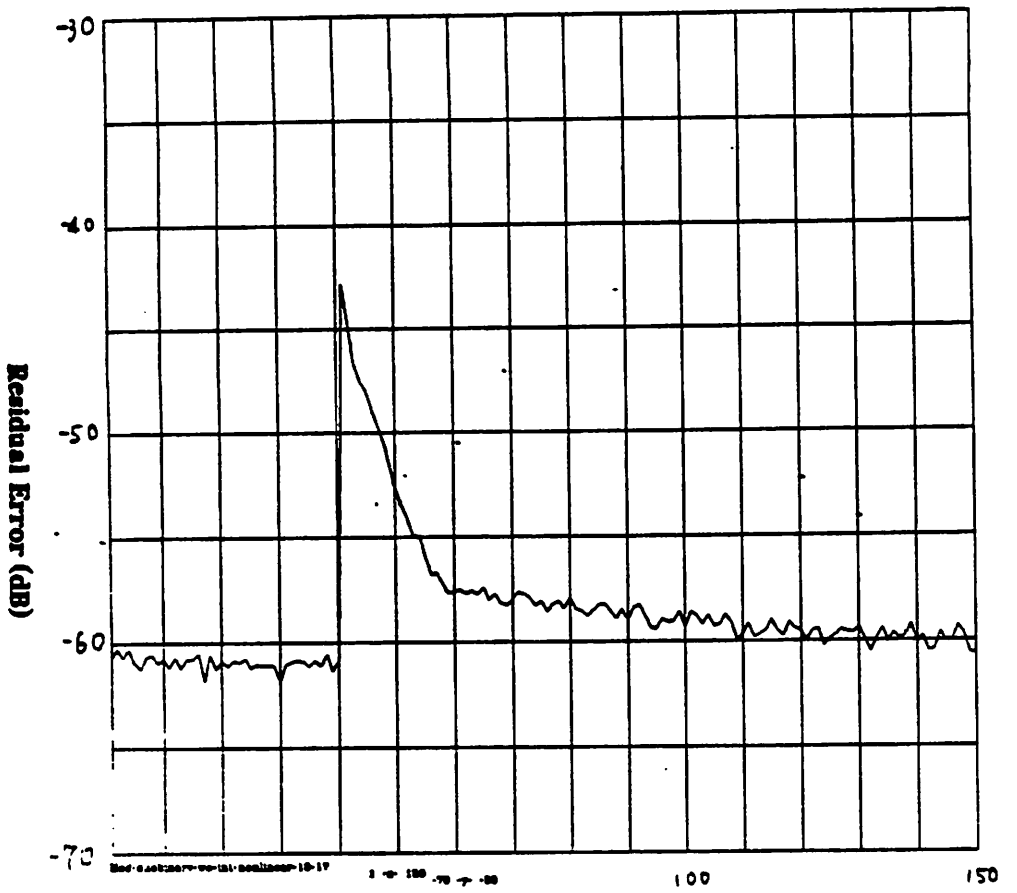

Figure 13(a). Jitter Performance of Nonlinear System
(Modified Binary PRC, No Interpolation)

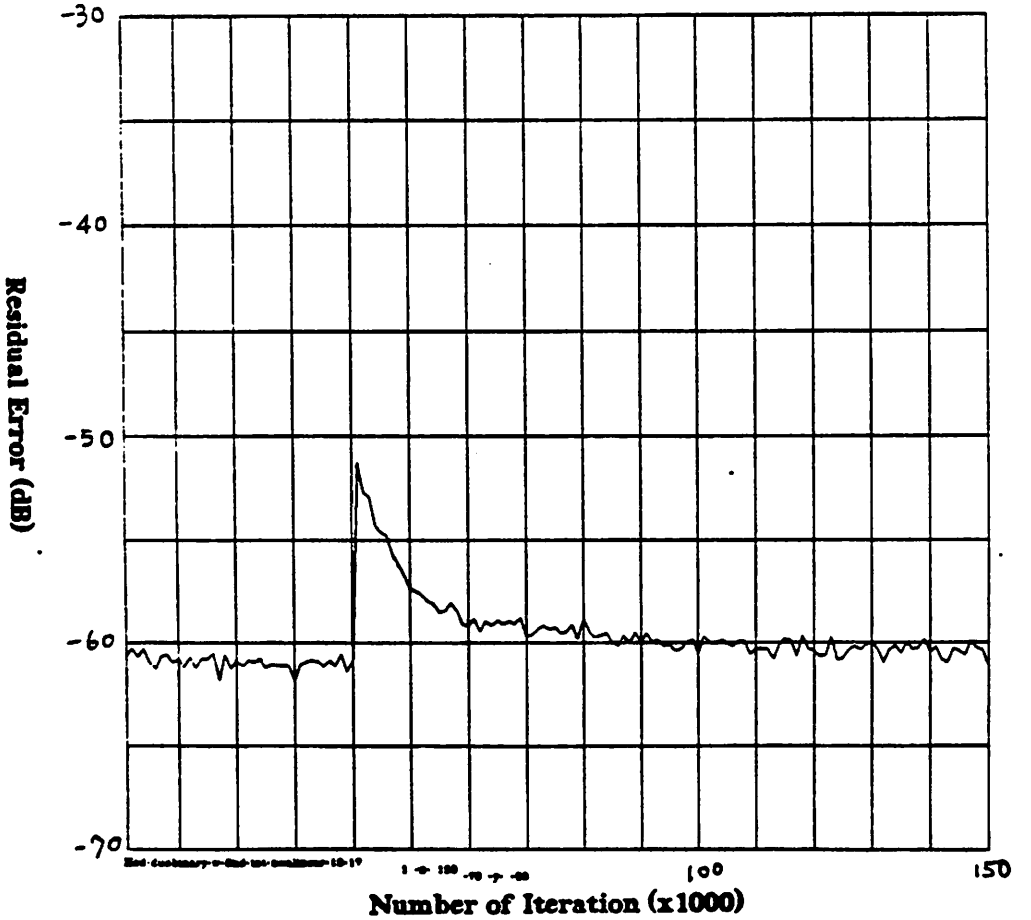

Figure 13(b). Jitter Performance of Nonlinear System
(Modified Binary PRC, 2nd Order Interpolation)

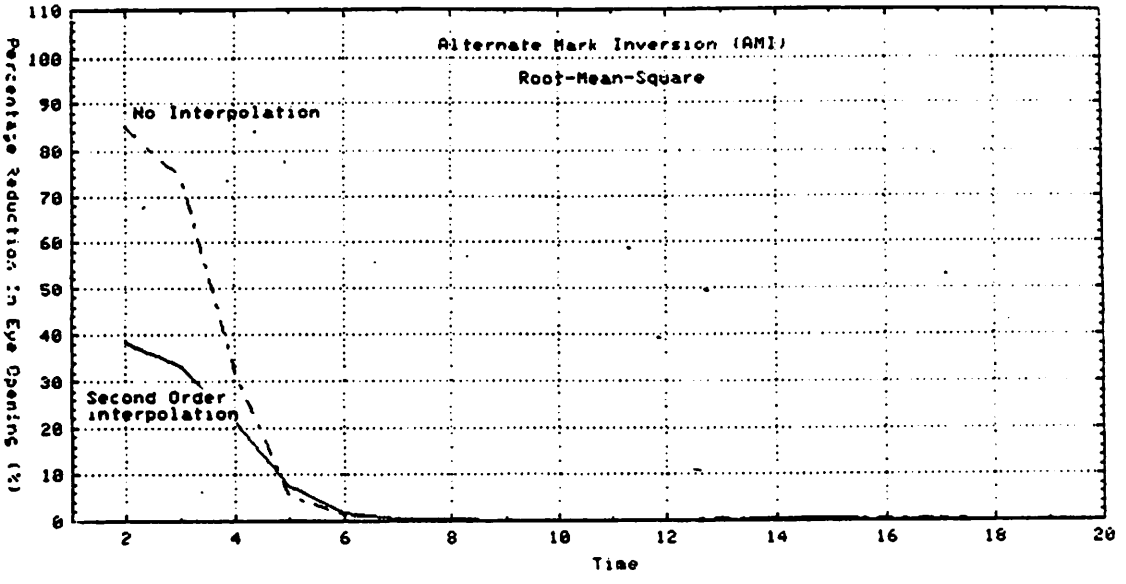

Figure 14(a). Jitter Performance, Transient Response (AMI, rms)

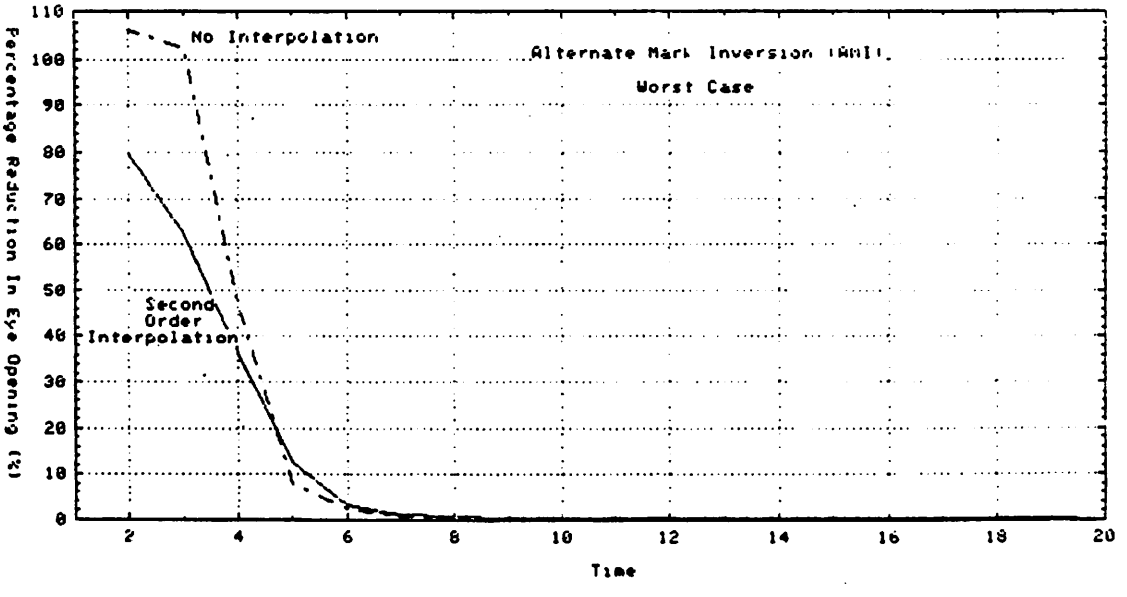

Figure 14(b). Jitter Performance, Transient Response (AMI, worst case)

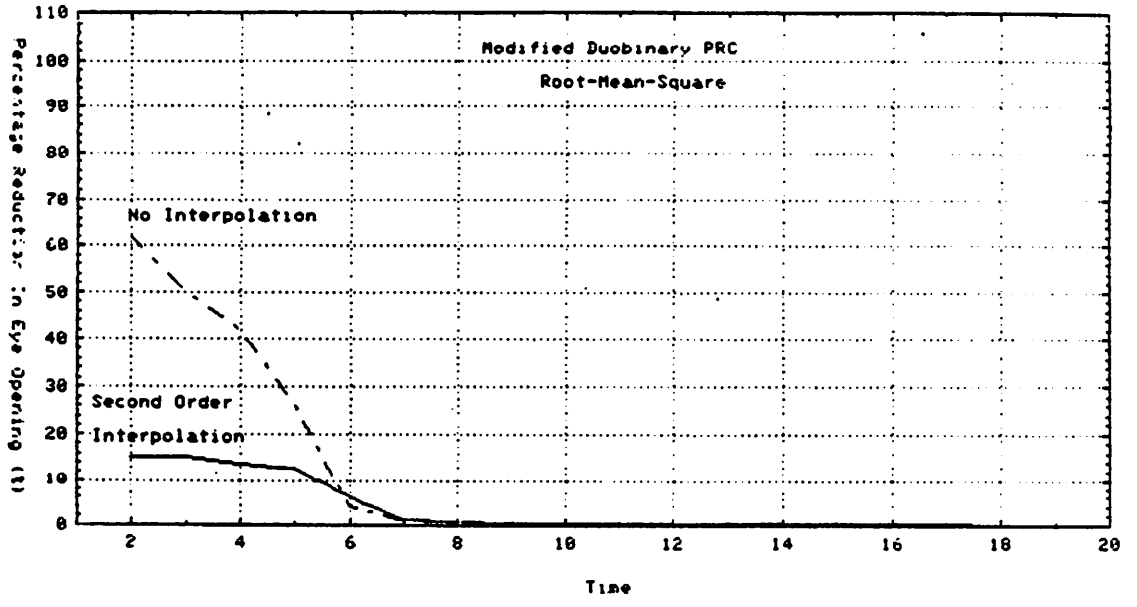

Figure 14(c). Jitter Performance, Transient Response (Modified Duobinary PRc, rms)

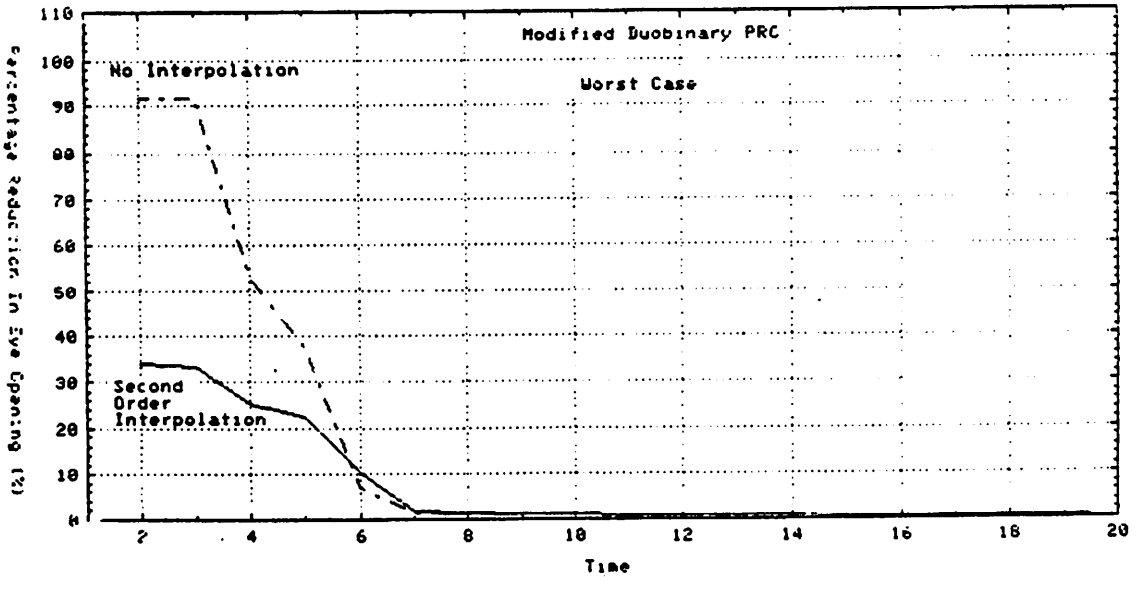

Figure 14(d). Jitter Performance, Transient Response (Modified Duobinary PRc, worst case)